PROTEINS
STRUCTURE ■ FUNCTION ■ BIOINFORMATICS

Free-energy computations identify the mutations required to confer trans-sialidase activity into *Trypanosoma rangeli* sialidase

Gustavo Pierdominici-Sottile,[1] Juliana Palma,[1] and Adrian E. Roitberg[2]*

[1] Departamento de Ciencia y Tecnología, Universidad Nacional de Quilmes, Saenz Peña 352, Bernal B1876BXD, Argentina

[2] Department of Chemistry and Quantum Theory Project, University of Florida, Gainesville, Florida 32611-7200

ABSTRACT

Trypanosoma rangeli's sialidase (TrSA) and Trypanosoma cruzi's trans-sialidase (TcTS) are members of the glycoside hydrolase family 33 (GH-33). They share 70% of sequence identity and their crystallographic C_α RMSD is 0.59 Å. Despite these similarities they catalyze different reactions. TcTS transfers sialic acid between glycoconjugates while TrSA can only cleave sialic acid from sialyl-glyconjugates. Significant effort has been invested into unraveling the differences between TrSA and TcTS, and into conferring TrSA with trans-sialidase activity through appropriate point mutations. Recently, we calculated the free-energy change for the formation of the covalent intermediate (CI) in TcTS and performed an energy decomposition analysis of that process. In this article we present a similar study for the formation of the CI in TrSA, as well as in a quintuple mutant ($TrSA_{5mut}$), which has faint trans-sialidase activity. The comparison of these new results with those previously obtained for TcTS allowed identifying five extra mutations to be introduced in $TrSA_{5mut}$ that should create a mutant ($TrSA_{10mut}$) with high trans-sialidase activity.

Proteins 2014; 82:424–435.

Key words: computational protein engineering; function-changing mutants; free energy; QMMM.

INTRODUCTION

Trypanosoma cruzi is the parasite responsible for Chagas' disease. Its infectivity in the human body depends on the enzyme trans-sialidase (TcTS),[1–5] which provides *T. cruzi* with the ability to adhere to the cells of the host and to evade its immune system.[6] It has been found that the parasite invasion is significantly reduced when the enzyme substrates are neutralized with antibodies.[7] Moreover, several studies describe the direct involvement of the enzyme in animal pathogenesis,[8] thymocyte apoptosis,[9] and induction of abnormalities in the host's immune system.[10] TcTS belongs to the CAZY GH33 family (www.cazy.org)[11,12] all of them sharing a similar catalytic domain, with a six-bladed β propeller topology.[13] This common motif and eight strictly conserved residues in the active site, strongly suggest a mutual evolutionary origin and a similar mode of action for the entire family.[14]

In particular, TcTS catalyzes the transfer of α-(2→3) sialic acid from sialoglycoconjugates to β-galactosyl glycoconjugates, with retention of configuration.[4] It can also have, under certain circumstances, a very small sialidase activity.[15] Kinetic isotope effect (KIE) experiments for TcTS have revealed a strong nucleophilic participation at the transition state (TS) that leads towards the covalent intermediate (CI) between the sialic acid and the enzyme.[16] Watts *et al.* were able to trap this CI using a substrate analog (deoxy-2,3-difluorosialic acid). They also identified Tyr342 as the nucleophile that attacks the anomeric C atom of sialic acid.[16,17]

Recently, we computed the free-energy profile describing the CI formation in the catalytic mechanism of TcTS with sialyl-lactose. KIE values were calculated and results were in good agreement with experimental

Additional Supporting Information may be found in the online version of this article.

Grant sponsor: National Institute of Health; Grant number: NIH 1R01AI073674-01; Grant sponsor: Large Allocations Resource Committee; Grant number: TG-MCA05T010; Grant sponsor: Consejo Nacional de Investigaciones Científicas y Técnicas (CONICET).

*Correspondence to: Adrian E. Roitberg, Department of Chemistry and Quantum Theory Project, University of Florida, Gainesville, P.O. Box 117200, FL 32611-7200. E-mail: roitberg@ufl.edu

Received 4 March 2013; Revised 26 July 2013; Accepted 14 August 2013
Published online 2 September 2013 in Wiley Online Library (wileyonlinelibrary.com).
DOI: 10.1002/prot.24408

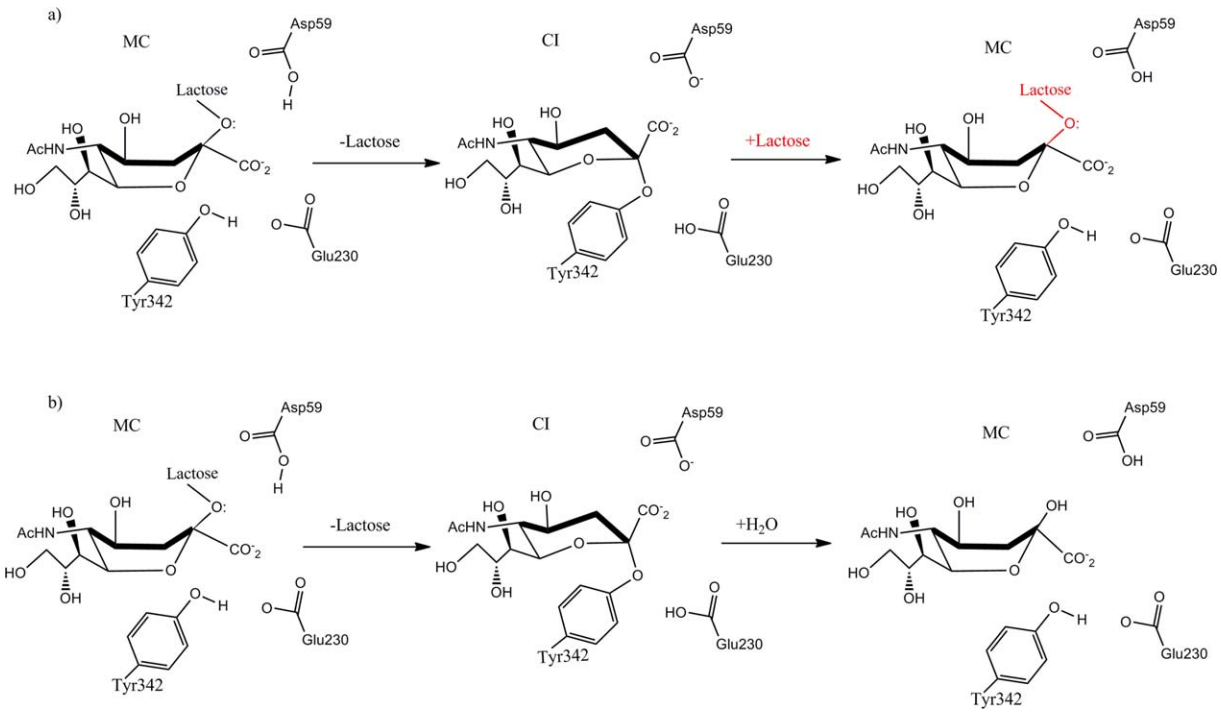

Figure 1

(**a**) Catalytic mechanism for TcTS. The first step involves reaching the CI configuration, the second one (reverse step) completes the reaction transferring the sialic acid to another lactose molecule (shown in red). (**b**) Catalytic mechanism for TrSA. In this case, once CI is reached, the reaction proceeds by hydrolysis of the sialyl-enzyme bond. [Color figure can be viewed in the online issue, which is available at wileyonlinelibrary.com.]

measurements. The analysis of the minimum free-energy path indicated that the estimated barrier ($(\Delta G_r^{\ddagger})$) for the reaction from the Michaelis complex (MC) to the CI was 20.8 kcal/mol. The computed (ΔG_r^0) was −0.89 kcal/mol. At the transition-state (TS) configuration, a strong nucleophilic participation and very little charge development at the anomeric C were found.[18]

Trypanosoma rangeli sialidase (TrSA), on the other hand, is a strict hydrolase, but shares 70% of sequence identity with TcTS. The comparison of the crystal structures of TcTS (PDB ID: 1MS3)[19] and TrSA (PDB ID: 1N1T)[13] shows that the overall C_α RMSD is just 0.59 Å[13] and that the active sites are surprisingly similar. Despite these similarities, TrSA is unable to act as trans-sialidase and can only cleave sialic acid from sialyl-glyconjugates, releasing it into the medium.[20] It has been shown that good inhibitors (DANA, Tamiflu) of TrSA and other sialidases are very weak inhibitors of TcTS. This makes the couple TcTS and TrSA an excellent system to understand how widely different catalytic activities can be attained with very similar structures.[21,22] In addition, unraveling the minute but vital differences between TcTS and TrSA could pave the way to tailor sialidases into trans-sialidases, and glycosidases into trans-glycosidases, to be employed in efficient synthesis of oligosaccharides with terminal sialic acids.

In Figure 1, the proposed mechanisms for TcTS and TrSA are illustrated. It is believed that both enzymes share the first half of the reaction (the transference of the sialic acid from the donor sugar to the enzyme (from MC to CI)). In TcTS, once the CI is reached the reaction proceeds taking the reverse step (i.e., going from the CI to MC) but transferring the sialic acid to an acceptor sugar. In TrSA however, a water molecule attacks the CI releasing sialic acid into the medium.

For the sake of simplicity, unless explicitly mentioned, we will number the residues according to the crystallographic structure of TcTS complexed with sialyl-lactose (PDB entry code: 1S0I).[23] These numbers do not match those in the crystallographic structure of TrSA but, instead, the homologous residues have to be considered. Mutations will always be mentioned by indicating first the TrSA residue and then the corresponding one in TcTS (i.e., Ser119-Tyr indicates that a Serine molecule that was at position 119 in TrSA was transformed into Tyrosine, which is the corresponding residue in TcTS).

In the active site of TcTS there are three catalytic residues (Tyr342, Asp59, and Glu230) plus another six residues that strongly interact with the substrate. This last group is made up by Asp96, which is hydrogen bonded to the sialic acid, the arginine triad—Arg35, Arg245, Arg314—which interacts with the carboxylate group of

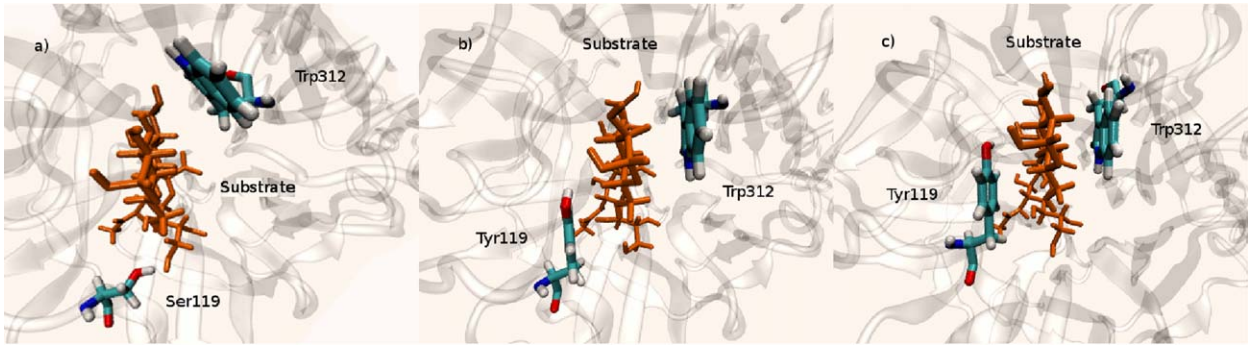

Figure 2

Configuration of the substrate (sialyl-lactose) in the active site of (**a**) TrSA, (**b**) TrSA5mut, and (**c**) TcTS. Residues Trp312 and Tyr119 (Ser119 for TrSA) are highlighted. In TrSA5mut and TcTS, the substrate is embraced by these two neighboring walls. In TrSA, there is only one wall (Trp312) and its configuration is twisted with respect to the lactose moiety. [Color figure can be viewed in the online issue, which is available at wileyonlinelibrary.com.]

the sialic acid, and the side chains of Trp312 and Tyr119, which lie parallel to each other and form the two lateral walls of the aglycon binding site of TcTS. The active site of TrSA shares the same description, except for the positioning of the lateral walls of the aglycon binding site. Tyr119 of TcTS is replaced by a serine residue in TrSA. The conformation of Trp312 in TrSA differs significantly from its conformation in TcTS.[13] In TrSA, the indol ring is placed in a position that precludes any π–π interaction with the sugar part of the substrate. Because of this, the active site of TcTS embraces the lactose part of the ligand quite differently than the active site of TcTS [see Fig. 2(a,c)] and the solvent exposure of the catalytic cleft in the ligand-bound for of TcTS is smaller than the corresponding one in TrSA.[24]

Taking advantage of the few differences between the active sites of TcTS and TrSA, a number of mutagenesis studies were performed to identify the amino acids required to confer trans-sialidase activity into TrSA.[13,15,21,25,26] However, this task turned out to be more challenging than one could think beforehand. A proof for this is given by the fact that none of the experiments performed so far has succeeded in producing a mutant with high trans-sialidase activity. In the first of such experiments, the substitution Ser119-Tyr was tried. However, the mutant failed to catalyze sialic acid transfer.[15] Interestingly, when the inverse mutation was performed on TcTS, the enzyme lost almost all its trans-sialidase ability.[25] These results indicate that the presence of Tyr119 is necessary, but not sufficient, to confer trans-sialidase activity into TrSA.

Other significant differences between the structures of these two enzymes appear at residues Pro283 and Tyr248 and therefore these positions were also tested as targets for mutagenesis experiments. In TcTS both residues lie side by side in two loops neighboring the Trp312 loop. There, they help to keep the indol group of Trp312 in a suitable conformation for substrate binding. In TrSA, however, these residues are replaced by glutamine and glycine, respectively. When the Gln283-Pro and Gln283-Pro/Gly248-Tyr mutations were tried on TrSA, it was found that the mutants did not acquire the ability to transfer sialic acid.[15] Trans-sialidase activity disappeared from TcTS when Pro283 was changed by Gln or when, in addition to this substitution, Tyr248 was replaced by Gly. Finally, the triple mutant of TrSA, Gly248-Tyr/Gln283-Pro/Ser119-Tyr was synthesized. Once again, the experiment failed to produce a mutant able to transfer sialic acid.[15] With the aim of modifying Asp96 immediate environment so as to mimic the one of TcTS, the next step was to supplement the three mutations mentioned above with two extra ones: Met95-Val and Ala97-Pro. This TrSA quintuple mutant ($TrSA_{5mut}$) presented a trans-sialidase activity that was only 1% of that found in wild-type TcTS. Finally, several sextuple mutants were tried ($TrSA_{6mut}$). Four of these mutants ($TrSA_{5mut}$ plus substitutions Val179Ala, Phe113Tyr, Thr38Ala, or Asp284Gly) showed activity similar to $TrSA_{5mut}$, while the other two sextuple mutants ($TrSA_{5mut}$ + Gly342-Ala or Ile36-Leu) presented roughly 11% of trans-sialidase activity [21]

Clearly, more substitutions have to be introduced to increase the trans-sialidase activity even further. However, selecting the locations for these new mutations is not a trivial task. There are 171 residues within a radius of 22 Å from the center of mass of the substrate in TcTS. Among these, 125 have the same identity in TcTS and in any of the $TrSA_{6mut}$ structures. This leaves just 46 locations to introduce new substitutions. Thus there are 46 different choices to design a $TrSA_{7mut}$, 1035 for a $TrSA_{8mut}$, 15180 for a $TrSA_{9mut}$, and 163185 for a $TrSA_{10mut}$. Obviously, the selection of the mutation sites is not performed at random. Instead, some physically sound criterion needs to be adopted to obtain an affordable number of choices. In

the former experiments, the location of the mutation sites was decided after a careful comparison of active sites between TcTS and TrSA. In this work we go one step further by introducing criteria based on quantum mechanics/molecular mechanics (QM/MM) molecular dynamics simulations. Particularly, we computed the free-energy profiles for the conversion of MC into CI in TrSA and $TrSA_{5mut}$, and compared these profiles with the previously reported one for TcTS.[18] These calculations were complemented with an energy decomposition analysis. The analysis highlights the individual contribution of each active site residue to the energy change of the reaction. Altogether, the results provide an explanation for the lack of trans-sialidase activity in TrSA and $TrSA_{5mut}$. Besides, they allow identifying five extra mutations to be introduced to $TrSA_{5mut}$ that would produce a mutant, $TrSA_{10mut}$, with the ability to transfer sialic acid. The evaluation of the free-energy for $TrSA_{10mut}$ shows a very similar profile to that found for TcTS, reinforcing the prediction of the energy decomposition analysis.

The methodologies applied in the different types of computations are described in the next section. After that, we present the results of the free-energy computations for TrSA and $TrSA_{5mut}$, and compare them with those of TcTS. This is followed by the presentation and discussion of the energy decomposition results. Finally we present the results of free-energy calculations for $TrSA_{10mut}$. The last section outlines the main conclusions of the work.

MATERIALS AND METHODS

General aspects

The crystallographic structure of TrSA complexed with DANA was used to model the structure of the enzyme in complex with sialyl-lactose (PDB entry code: 1N1T). DANA is a structural analog of the sialic acid oxocarbenium ion and an efficient inhibitor for TrSA and sialidases in general.[22] To find the initial coordinates of the lactose group of the substrate we superimposed DANA with the sialyl-lactose moiety found in the crystal structure of the Michaelis complex in TcTS (PDB entry code: 1S0I). The resultant coordinates of the sialyl-lactose, together with those of the TrSA atoms were used as the starting geometry of TrSA in the MC form. It should be noted that this procedure produces a different orientation for the indol ring of Trp312 with regard to the lactose group than the one found in TcTS (see Fig. 2). Recently, Mitchell *et al.* found that Trp312 in TcTS acts as a shovel when the lactose moiety moves from or into the active site.[27] Something similar could happen in TrSA. However, this movement takes place after the MC to CI conversion and before the following CI to MC one. Therefore it is out of the scope of the present work.

Along this work, we thoroughly compare the results of MD simulations of TrSA with those of TcTS reported previously.[18] Also, the sequences and structures of both enzymes are set against each other. It is thus important to mention that, while the crystal structure of TrSA used in this work was obtained in its wild-type form, that of TcTS (PDB code: 1S0I) was obtained upon introducing eight mutations. These mutations are: Asn58-Phe, Asp59-Ala, Ser495-Lys, Val496-Gly, Glu520-Lys, Asp593-Gly, Iso597-Asp, and His599-Arg. To analyze the dynamics of TcTS in the wild-type form, these eight mutations were reverted before carrying out the computations reported in Ref. 18. To make this point clearer, we present in the Supporting Information section an alignment between the sequences of TrSA and TcTS whose structures and dynamics are compared along this work.

The leap module of the AMBER10 molecular dynamics package[28] was used to add the necessary hydrogen atoms and to solvate the system in a truncated octahedral cell of TIP3P[29] explicit water molecules. The ff99SB[30,31] and Glycam04[32,33] force fields were used to construct the topology files. In all QM/MM simulations, the self-consistent charge Density Functional Tight Binding (scc-DFTB) method,[34] as implemented in AMBER10,[35] was used to describe the potential energy of the QM subsystem. This method has proven itself suitable for describing the energetics of chemical[36] and biochemical reactions.[18,37] It has also been shown to provide the best semiempirical description for six-member carbohydrate ring deformation.[38,39] All the molecular dynamics simulations utilized different pseudorandom seeds as recommended by Sindhikara *et al.*[40] and the QM subsystem, which involved 176 atoms, was always defined as the substrate plus residues Asp63, Tyr346, Glu234, Arg39, and Arg249. It is to be noticed that the numbers given, in this case, are the same as those in the TrSA structure (numbers for TcTS are Asp59, Tyr342, Glu230, Arg35, and Arg245).

All systems studied in this work were initially minimized. Then, they were heated during 50 ps from 0 K to a target temperature of 300 K, under constant volume conditions with $\tau_{tp} = 2.5$ ps. Afterwards we performed an equilibration stage of 80 ps at constant temperature and pressure, keeping both τ_{tp} and τ_p at 2.0 ps. Configurations from the heating and equilibration stages, sampled every 1 ps, were used to assess the evolution of the RMSD of the heavy atoms with respect to the initially minimized structure. In all cases we observed that the systems reached a converged RMSD smaller than 2.5 Å before 20 ps.

$TrSA_{5mut}$ generation

Once the TrSA in complex with sialyl-lactose was generated, it was used as the starting point to obtain the quintuple mutant ($TrSA_{5mut}$: Met95-Val, Ala97-Pro, Ser119-Tyr, Gly248-Tyr, and Gln283-Pro) studied by Paris *et al.*[21] Among these five *in silico* mutations,

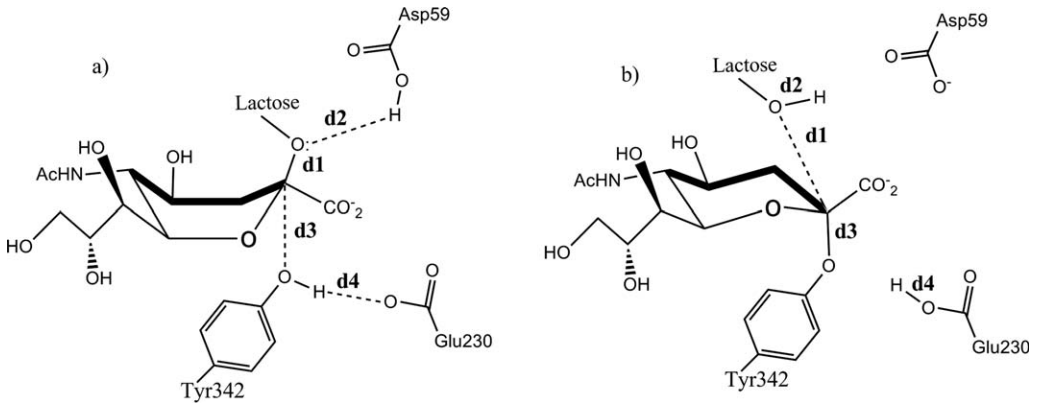

Figure 3

Distances employed to examine the 2D reaction coordinate. d1 represents the distance between the anomeric C of sialic acid and the glycosidic O of lactose; d2 accounts for the distance between the acidic H of Asp59 and the glycosidic O of lactose; d3 is the distance between the anomeric C of the sialic acid and the hydroxyl O of Tyr342 and d4 describes the distance between one carboxyl O of Glu230 and the hydroxyl H of Tyr342. In panel (**a**), the MC configuration is considered while in panel (**b**), the CI configuration is shown.

Ser119-Tyr and Gln283-Pro deserve special attention. The aromatic ring of Tyr119 lies parallel to the lactose ring of the substrate in the MC complex of TcTS. Thus, the Ser119-Tyr mutation was performed by adding the tyrosine atoms into the TrSA structure in a way that mimics the configuration found in TcTS. Upon making the Gln283-Pro substitution we modified the dihedral angles χ_1 and χ_2 of Trp312 since experiments show that this mutation forces the side chain of Trp312 to adopt an orientation parallel to the lactose ring.[21] Accordingly, the angles χ_1 and χ_2 were changed from their values in TrSA to those in TcTS (see Fig. 2).

Umbrella sampling calculations

Reaction coordinates were defined using the distances depicted in Figure 3: d1 represents the distance between the anomeric C of sialic acid and the glycosidic O of lactose, d2 accounts for the distance between the acidic H of Asp59 and the glycosidic O of lactose, d3 is the distance between the anomeric C of the sialic acid and the hydroxyl O of Tyr342; and d4 describes the distance between one carboxyl O of Glu230 and the hydroxyl H of Tyr342.

To investigate the formation of the CI in the mechanism of TrSA we explored a 2D free-energy profile using the reaction coordinates RC1 = d1 − d2 and RC2 = d3 + d4. These are the same employed to study the path from the MC to the CI in TcTS.[18]

RC1 was sampled from −0.21 Å to 3.07 Å while RC2 was sampled between 4.77 Å to 2.37 Å. Both scannings were made in steps of 0.08 Å. In each window a 25 ps. QM/MM MD was performed after a 10 ps period of equilibration. The 2D weighted histogram analysis method (WHAM-2D)[41] implemented in the package written by Alan Grossfield, was used to analyze the probability density and to obtain the free-energy profiles along the reaction coordinates for the unbiased system. The same 2D scan was done for $TrSA_{5mut}$ and $TrSA_{10mut}$. RC1 was sampled from −0.31 Å to 2.97 Å in $TrSA_{5mut}$ and from −0.23 Å to 2.89 Å in $TrSA_{10mut}$, while RC2 was scanned from 4.97 Å to 2.41 Å in the quintuple mutant and from 4.85 Å to 2.37 Å in $TrSA_{10mut}$. Statistical uncertainties for each point were calculated with a Monte Carlo bootstrap error analysis,[42] as implemented within the WHAM program. Convergence of the free-energy profiles was tested considering 1D umbrellas sampling fixing RC1 at one value and scanning RC2, or vice versa. For these cases, 75 ps. QM/MM MD simulations were performed in each window and the free energy results were compared to those obtained considered the data used in the 2D scan.

Energy decomposition

We have utilized an energy decomposition analysis to evaluate how the active site residues, individually, stabilize/destabilize the CI with respect to the MC in TcTS, $TrSA_{5mut}$, and $TrSA_{10mut}$. A similar approach was recently applied by Lin *et al.* to investigate an internal proton transfer step in Dopa decarboxylase[43] and by us to understand the changes in the free-energy profiles for the proton transfer between Tyr342 and Glu230, observed upon substrate binding in TcTS.[44] Different variations of this approach have been extensively used with other enzymatic reactions.[45–52] The details of the energy decomposition analysis employed in this work are explained in the following paragraphs.

We will denote the quantum Hamiltonian as H_{QM} the wave function describing the quantum subsystem in the presence of the classical environment as $|\Psi\rangle$ and the wave function for the quantum subsystem in the gas phase as $|\Psi\prime\rangle$ Considering this, the energy change for the

transformation from MC to CI in gas phase ($(\Delta E^{QM}_{MC\to CI})$) can be mathematically expressed as,

$$\Delta E^{QM}_{MC\to CI} = \langle \Psi'_{CI}|H_{QM}|\Psi'_{CI}\rangle - \langle \Psi'_{MC}|H_{QM}|\Psi'_{MC}\rangle. \quad (1)$$

Similarly, the energy change in the presence of the classical environment ($\Delta E^{QM/MM}_{MC\to CI}$) is,

$$\Delta E^{QM/MM}_{MC\to CI} = \left\langle \Psi_{CI}\left| H_{QM} + \sum_i V_i \right| \Psi_{CI}\right\rangle - \langle \Psi_{MC}| H_{QM} + \sum_i V_i \left| \Psi_{MC}\right\rangle, \quad (2)$$

where $\Sigma_i V_i$ denotes the non-bonded interaction of each residue in the classical region with the quantum subsystem. Taking the difference between Eqs. (2) and (1), we can quantify the influence of the environment in the energy change of the reaction ($\Delta\Delta E^{MMinf\,lu}_{MC\to CI}$) as,

$$\Delta\Delta E^{MMinf\,lu}_{MC\to CI} = \Delta E^{QMMM}_{MC\to CI} - \Delta E^{QM}_{MC\to CI} = \Delta E_{CI} - \Delta E_{MC} + \sum_i (\langle \Psi_{CI}|V_i|\Psi_{CI}\rangle - \langle \Psi_{MC}|V_i|\Psi_{MC}\rangle) \quad (3)$$

where $\Delta E_{CL} = \langle \Psi_{CL}|H_{QM}|\Psi_{CI}\rangle - \langle \Psi'_{CL}|H_{QM}|\Psi'_{CI}\rangle$ and $\Delta E_{MC} = \langle \Psi_{MC}|H_{QM}|\Psi_{MC}\rangle - \langle \Psi'_{MC}|H_{QM}|\Psi'_{MC}\rangle$ measure how the expectation energies of CI and MC are modified by changes in the wave function. None of these values can be ascribed to any single residue. They are rather caused by the whole protein environment. Since $|\Psi'_{CI}\rangle$ and $|\Psi'_{MC}\rangle$ are eigenfunctions of H_{QM} both ΔE_{CI} and ΔE_{MC} have positive values and tend to cancel each other in Eq. (3). On the other hand, each term appearing within the sum of Eq. (3) measures the individual contribution of a particular residue to the energy change of the reaction. We will denote these terms as ($\Delta E^{i}_{MC\to CI}$). Thus,

$$\Delta E^{i}_{MC\to CI} \equiv \langle \Psi_{CI}|V_i|\Psi_{CI}\rangle - \langle \Psi_{MC}|V_i|\Psi_{MC}\rangle. \quad (4)$$

We have used these $\Delta E^{i}_{MC\to CI}$ values to assess the effect of individual residues on $\Delta\Delta E^{MMinf\,lu}_{MC\to CI}$. To calculate $\langle \Psi_X|V_i|\Psi_X\rangle$, we considered that:

$$\langle \Psi_X|V_i|\Psi_X\rangle = \langle \Psi_X|H_{QM} + \textstyle\sum_i V_i|\Psi_X\rangle - \langle \Psi_X|H_{QM} + \sum_{j\neq i} V_j|\Psi_X\rangle, \quad (5)$$

with X = MC or CI. The first term of Eq. (5) gives the total energy of the system in a given configuration while the second is a fictitious energy calculated using the same wave function and environment, except for the i-th residue which is transformed into Gly. These fictitious energies were computed with a modified version of Amber 10.

It should be noticed that the partition between quantum and classical subsystems applied in these computations was different than that used to run the MD calculations. In particular, the quantum subsystem was defined as the substrate plus residues Asp59, Tyr342, and Glu230. The rest of the enzyme was assigned to the classical subsystem. Average values of $\langle \Psi_{MC}|V_i|\Psi_{MC}\rangle$ and $\langle \Psi_{CI}|V_i|\Psi_{CI}\rangle$ were evaluated through applying Eq. (5) to 125 snapshots taken from the Umbrella Sampling calculations of the MC and CI configurations and taking the average. These data were then used to compute average values of $\langle \Psi_X|V_i|\Psi_X\rangle$ for all the residues lying within a sphere of radius 10.0 Å, centered at the center of mass of the QM subsystem. This procedure selects 75 residues for both, TcTS and the mutants of TrSA. We have found that residues lying outside this sphere have negligible values of $\Delta\Delta E^{MMinf\,lu}_{MC\to CI}$

RESULTS AND DISCUSSION

Minimum free-energy profiles

The 2D free-energy contour plots for the transformation between MC and CI in the catalytic mechanism of TrSA, $TrSA_{5mut}$, and TcTS are shown in Figure 4. Results for TcTS were taken from Ref. [18]. The minimum free-energy path is highlighted with a white dashed line. Figure 5 shows the free energies for the MC (MC′), TS (TS′), and CI, for the systems under study. In both figures, the zero of energy was set at the MC configuration. It is noteworthy that the most important parameters in Figure 5 are the free-energy barriers for the conversion from CI to MC′, since this is the step required for trans-sialidase activity. Accordingly, the numerical values of these barriers were indicated in the picture. Other relevant parameters, as the barriers for the conversion from MC to CI, its (ΔG^0_r) and distance d3 at the MC and TS configurations (see Fig. 3), are presented in Table I.

In TrSA and $TrSA_{5mut}$, the barriers to reach CI are about 5.0 kcal/mol smaller than in TcTS while the ($\Delta G^0_r s$) are nearly 10.0 kcal/mol lower (see Fig. 5). This indicates that the environments of TrSA and $TrSA_{5mut}$ selectively stabilize the CI conformation with respect to the MC one, while the environment of TcTS does not (note that (ΔG^0_r) for TcTS is nearly zero). These facts provide a seemingly valid explanation for the lack of trans-sialidase activity in TrSA. Once CI is reached, trans-sialylation requires that the reverse step (transferring the sialic acid to a different lactose molecule) can take place fast enough to avoid alternative reactions. In TcTS, the forward and reverse barriers are almost the same (~20.80 kcal/mol) but in TrSA the barrier for the reverse step gets significantly higher (26.1 ± 1.55 kcal/mol) because of the CI stabilization. Therefore, the reverse step in TrSA becomes slower and hydrolysis occurs first. With a barrier for the reverse reaction of 24.8 kcal/mol, the situation found in $TrSA_{5mut}$ is energetically similar to that of TrSA, rather than to TcTS. This fact explains its low trans-sialidase activity. Within the framework of classical transition state theory the

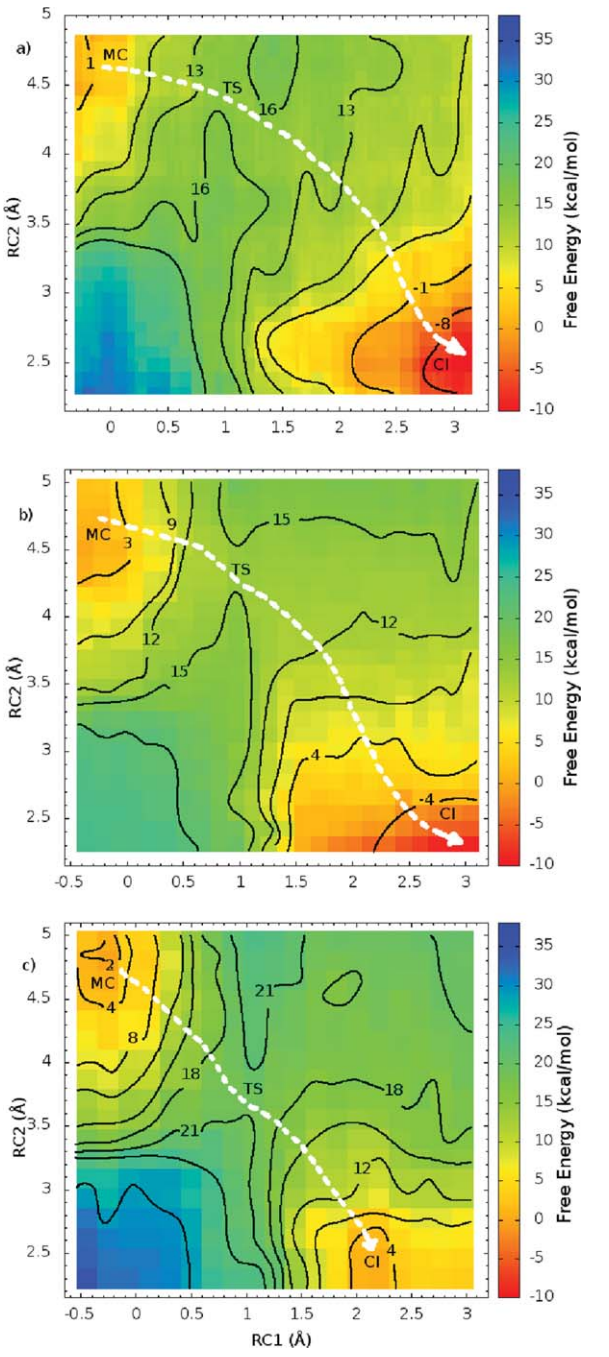

Figure 4

Free-energy contour plots for the MC to CI transformation in TrSA (**a**), $TrSA_{5mut}$ (**b**), and TcTS (c), using sialyl-lactose as substrate. Energies are given in kcal/mol. The white-dashed lines indicate the minimum free-energy path.

calculated barriers predict that the ratio $k^{CI\rightarrow MC'}_{TrSA\_Smut}/k^{CI\rightarrow MC'}_{TcTS}$ for the kinetic constants of the CI to MC′ conversion, should be 0.045 at 298 K. This small value is very close to the trans-sialidase activity experimentally found for $TrSA_{5mut}$, which was 1% of the wild-type TcTS activity.[21]

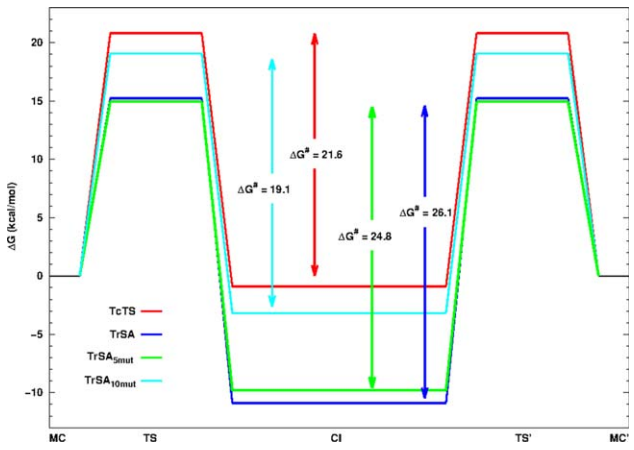

Figure 5

Free-energy profiles for the trans-sialylation reaction in TcTS (red line), TrSA (blue line), $TrSA_{5mut}$ (green line), and $TrSA_{10mut}$ (light blue line). Energies are given in kcal/mol. Note that once the CI configuration is reached, trans-sialylation is completed by taking the reverse step [from the CI to another MC with a new acceptor sugar (MC′)]. [Color figure can be viewed in the online issue, which is available at wileyonlinelibrary.com.]

Another important difference between TcTS and TrSA/$TrSA_{5mut}$ is the configuration of the TS. The value of the reaction coordinate RC2 (d3 + d4) at the TS is ~4.5 Å for TrSA and the quintuple mutant, but it plummets to ~3.5 Å in TcTS. This difference is mainly due to the change in d3 which is almost the same for the three systems at the MC configuration, but is considerably shorter at the TS in TcTS (see Table I). This result indicates a higher flexibility of Tyr342 in TcTS than in TrSA and is in agreement with the observations of Paris *et al.*[13,17,19] who suggested that this difference could be related to the lack of trans-sialidase activity of TrSA.[21] Besides, the fact that the value of d3 at TS in $TrSA_{5mut}$ is similar to that of TrSA shows that the five mutations are not enough to change the flexibility of Tyr342.

The last paragraph highlights the similarities between the active sites of TrSA and $TrSA_{5mut}$ as compared to the one of TcTS. However, it is worth noticing that the active sites of $TrSA_{5mut}$ and TcTS share some common features and that these features contrast with those of

Table I

Parameters Characterizing the MC to CI Transformation in TrSA, $TrSA_{5mut}$, and TcTS

Parameters	TrSA	$TrSA_{5mut}$	TcTS
$\Delta G_r^{\ddagger}$(kcal/mol)	15.23 ± 0.87	14.95 ± 0.4	20.80 ± 0.7
(ΔG_r^0) (kcal/mol)	−10.87 ± 0.68	−9.81 ± 0.54	−0.89 ± 0.43
d3 at MC (Å)	3.49 ± 0.14	3.41 ± 0.11	3.39 ± 0.15
D3 at TS (Å)	3.03 ± 0.11	2.92 ± 0.08	2.52 ± 0.10

Free-energy barrier $\Delta G_r^{\ddagger}$ and free-energy change $(\Delta G_{\downarrow} r^{\uparrow} 0)$ for the transformation between MC and CI in TrSA, $TrSA_{5mut}$, and TcTS, along with the d3 distance at the MC and TS configurations (see Fig. 3). Results for TcTS were taken from Ref. [18].

native TrSA. For example, the side chain of Glu283 in TrSA is H-bonded to the lactose part of the substrate in ~60% of the configurations along the minimum free-energy path. In $TrSA_{5mut}$ this residue is changed to Pro and instead of interacting with the substrate remains close to Trp312, a situation that resembles that found in TcTS. Moreover, while the orientation of Trp312 is similar in $TrSA_{5mut}$ and TcTS, it differs from that observed in native TrSA. Along the minimum free-energy path of each system, the average distances stretching from the center of mass of the indol group of Trp312 to the glucose moiety of the substrate are 7.63 ± 0.76 Å for TrSA, 4.46 ± 0.18 Å for TcTS, and 3.81 ± 0.30 Å for $TrSA_{5mut}$. Furthermore, for the three systems, the dihedral angles of Trp312 oscillate around their initial values, indicating that the original configuration of Trp312 is maintained during the whole conversion between MC and CI.

Summarizing, the previous analysis shows that the mutations performed to obtain $TrSA_{5mut}$ introduce significant changes in the structure of the active site. However, they do not produce a minimum free-energy path similar to that found in TcTS. These mutations neither seem to help the nucleophile, Tyr342, and the anomeric C, to be brought closer, nor help to get a (ΔG_r^0) similar to that of TcTS. Clearly, new substitutions intended to produce a mutant with high trans-sialidase activity should address this point.

To increase the nucleophile participation at the TS the substitutions Ile36-Leu and Gly341-Ala are proposed. Both residues are closed to Tyr342, the residue whose configuration needs to be changed. We note that these two mutations have already been tried experimentally (but separately) on $TrSA_{5mut}$, producing two different $TrSA_{6mut}$ structures with about 11% of trans-sialidase activity.[21] This experimental finding confirms that the mutations are helpful. However, it also hints at the fact that more changes are needed to create a mutant with high trans-sialidase activity. Such changes should be selected according with their ability to modify the of the (ΔG_r^0) reaction.

Energy decomposition

We contrasted the patterns of stabilization of CI with regard to MC (measured by $\Delta E^i_{MC\to CI}$) for the active site residues of TcTS and $TrSA_{5mut}$. In so doing, our aim was to identify extra substitutions that would produce a mutant with a (ΔG_r^0) similar to that of TcTS. In Table II, we list the values of $\Delta E^i_{MC\to CI}$ for the most influential residues, considering that this influence is assessed by large and positive values of $\Delta\Delta E^{TrSA-TrSA_{smut}}_{MC\to CI}$. Note that a positive value of $\Delta\Delta E^{TrSA-TrSA_{smut}}_{MC\to CI}$ indicate a stronger stabilization of the CI with respect to the MC in the mutant than in TcTS, a feature that hinders transialidase activity.

The first two lines of Table II show positions for which the residues in TcTS and $TrSA_{5mut}$ differ. At position 58 TcTS has Asn while $TrSA_{5mut}$ has Phe. At position 284 TcTS has Gly while $TrSA_{5mut}$ has Asp. In both cases, the residues stabilize CI over MC in $TrSA_{5mut}$ while their effect is neutral or destabilizing of CI in TcTS. Since stabilization of CI hinders trans-sialidase activity, we suggest introducing the Phe58-Asn and Asp284-Gly mutations in $TrSA_{5mut}$. The addition of the Asp284-Gly mutation to $TrSA_{5mut}$ was experimentally tried by Paris *et al.*, who did not observe a significant increase in trans-sialidase activity.[21] On the other hand, as far as we know, the effect of the Phe58-Asn mutation has not been experimentally tested yet.

Table II
Stabilization Pattern of the CI with Respect to the MC for Influential Residues of TcTS and $TrSA_{5mut}$

TcTS	$TrSA_{5mut}$	$(\Delta E^i_{MC\to CI})$ TcTS	$(\Delta E^i_{MC\to CI})$ $TrSA_{5mut}$	$\Delta\Delta E^{TrSA-TrSA_{smut}}_{MC\to CI}$
Gly284	Asp284	0.00	−4.43	4.43
Asn58	Phe58	3.16	−0.63	3.79
Trp312	Trp312	1.42	−4.25	5.67
Asp96	Asp96	2.88	−2.28	5.16
Glu357	Glu357	1.81	−2.50	4.31

The values for the relative stabilization of the CI with respect to the MC [see Eq. (4)] for the most influential active site residues. The results for all the residues analyzed are shown in the Supporting Information. Energies are given in kcal/mol. The last column shows the differences between the figures presented in columns 3 and 4 (in all cases the standard deviations are <0.6 kcal/mol).

The following three rows of Table II show the values for residues which are the same in both systems. These are Trp312, Asp96, and Glu357. The large values of their $\Delta\Delta E^{TrSA-TrSA_{smut}}_{MC\to CI}$ point to the fact that their interaction with the QM subsystems of both enzymes is significantly different. This can be attributed to a different positioning of the residues with regard to the QM subsystem. Accordingly, a strategy to confer trans-sialidase activity to the mutant should be adding extra mutations aimed at modifying the surroundings of these residues, so as to make them similar to those found in TcTS. We note, however, that four of the five mutations introduced into TrSA to produce $TrSA_{5mut}$ were aimed at altering the surroundings of Asp96 and Trp312.[21] Therefore there is little left to be done in that regard, but a new mutation can be introduced to change the positioning of Glu357. With this goal in mind, the substitution Thr38-Ala was proposed since a change at position 38 would help to modify the conformation of Pro37, which is in close contact with Glu357. It should be noted that the effect of Ala38 and Pro37 is nondirect. These two residues are outside the sphere of 10.0 Å used in the energy decomposition analysis. Ala38, for example, is 21.8 Å away from the center of mass of the substrate. Therefore, they have negligible values of $\Delta\Delta E^{TrSA-TrSA_{smut}}_{MC\to CI}$ However, they exert an important influence on the conformation of Glu357 which, in turn, has a large and positive value of $\Delta\Delta E^{TrSA-TrSA_{smut}}_{MC\to CI}$ The Thr38-Ala mutation was also

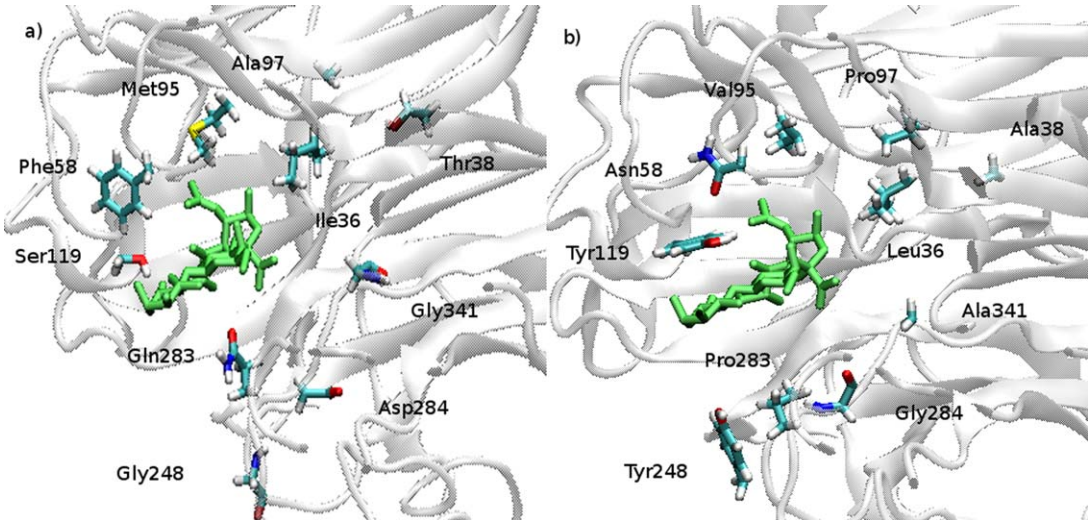

Figure 6

(**a**) Active site of TrSA and TcTS (**b**) highlighting the residues proposed to convert TrSA wild type in $TrSA_{10mut}$. [Color figure can be viewed in the online issue, which is available at wileyonlinelibrary.com.]

experimentally tried on $TrSA_{5mut}$ and was found to increase its trans-sialidase activity from 1 to 6.4%.[21]

$TrSA_{10mut}$

According to the discussion of the previous sections, we introduced five mutations into $TrSA_{5mut}$ to obtain an *in-silico* mutant, $TrSA_{10mut}$, with high trans-sialidase activity. Two of them (Ile36-Leu and Gly341-Ala) can be labeled as "structural" as were proposed to have a similar participation of the nucleophile at the TS. The other three substitutions (Phe58-Asn, Asp284-Gly, and Thr38-Ala) can be labeled as "energetic" since they were proposed to obtain a mutant with a (ΔG_r^0) similar to that of TcTS and were selected according to the energy decomposition analysis. Employing the numbering of TrSA numbering, these mutations would be Ile40-Leu, Gly345-Ala, Phe62-Asn, Asp288-Gly, and Thr42-Ala. As already stated above, four of these five substitutions were already experimentally tried individually, and were found to yield mutants with low to moderate trans-sialidase activity. The criterion used to experimentally test these mutations was basically based on crystallographic information and the fact that we have also proposed these substitutions (based on structural and energetic criteria) is a great convergent result. On the other hand, as far as we know, the mutation Phe58-Asn has not been tried yet, not has $TrSA_{10mut}$ (with the substitutions proposed here) ever been synthesized or tested. It is important to remark that most, if not all, TcTS crystallographic structures were obtained introducing mutations on positions 58, but in its wild-type form this residue is an asparagine. Figure 6 shows the active sites of the wild-type forms of TcTS and TrSA, highlighting the mutations sites proposed for $TrSA_{10mut}$.

To confirm that the proposed substitutions have the desired effect we computed the free-energy surface for the conversion from MC to CI in $TrSA_{10mut}$. The result is shown in Figure 7. The barrier for the direct process, being 16.0 ± 0.6 kcal/mol, is smaller than that found in TcTS (20.8 kcal/mol). The calculated (ΔG_r^0) is −3.2 ± 0.6 kcal/mol, demonstrating that the stabilization of the CI conformation does not resemble that found in $TrSA_{5mut}$ but is, instead, similar to that of TcTS (∼ −0.9 kcal/

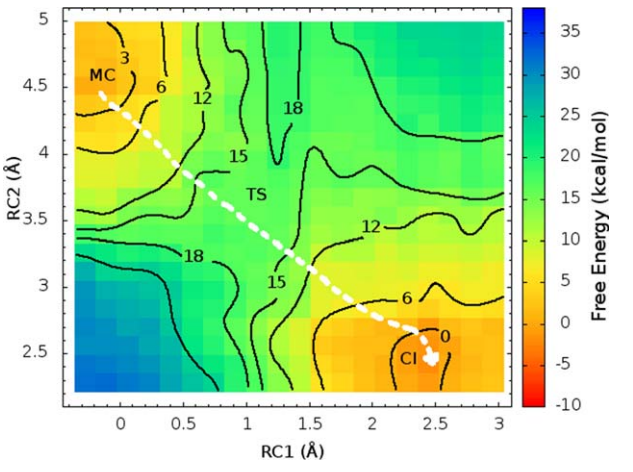

Figure 7

Free-energy contour plots for the MC to CI transformation in $TrSA_{10mut}$ using sialyl-lactose as substrate. Energies are given in kcal/mol. The white-dashed line indicates the minimum free-energy path. [Color figure can be viewed in the online issue, which is available at wileyonlinelibrary.com.]

Table III
Stabilization Pattern of the CI with Respect to the MC for the Most Influential Residues of $TrSA_{10mut}$

$TrSA_{10mut}$	$(\Delta E^{i}_{MC\rightarrow CI})$	$\Delta\Delta E^{TrSA-TrSA_{10mut}}_{MC\rightarrow CI}$
Gly284	0.0	0.0
Asn58	1.26	1.90
Trp312	1.02	0.40
Asp96	−1.61	4.49
Glu357	0.82	0.99

The values for the relative stabilization of CI with respect to MC [see Eq. (4)] for the most influential active site residues of $TrSA_{10mut}$. The results for all the residues analyzed are shown in the Supporting Information. Energies are given in kcal/mol. The last column shows the differences of the values of column two and those of TcTS, given in the third column of Table II. In all cases, the standard deviations are <0.75 kcal/mol.

mol). Therefore, once CI is reached in $TrSA_{10mut}$ the reverse step requires surmounting a barrier of 19.1 kcal/mol, a value close to the one found in TcTS, and significantly smaller than that of TrSA (see Fig. 5). Thus, according to classical transition state theory, the trans-sialylation reaction in TcTS and $TrSA_{10mut}$ should occur at similar rates. It is worth noting, however, that this condition is not enough to assure a comparable trans-sialidase activity since such activity depends on the competition of two processes: trans-sialylation and hydrolysis. This work has only focused on the trans-sialylation reaction.

An inspection of the structure of $TrSA_{10mut}$ along the minimum free-energy path shows that the nucleophile participation at the TS, characterized by distance d3, is 2.48 ± 0.13 Å, a value really close to that found in TcTS (2.52 ± 0.10 Å). Since this nucleophile participation is seen in $TrSA_{10mut}$ but not in $TrSA_{5mut}$, we conclude that the last five mutations are responsible for the change. As explained above, probably the main effect is due to the Ile36-Leu and Gly341-Ala substitutions, which are close neighbors of the nucleophile Tyr342.

Finally, we also applied the energy decomposition analysis to $TrSA_{10mut}$. The results are presented in Table III. Since all the extra mutations were proposed to reduce the CI stabilization over the MC, one wosuld expect that the values of $\Delta\Delta E^{TrSA-TrSA_{5mut}}_{MC\rightarrow CI}$ in Table III were smaller than the corresponding ones in Table II. This is in fact what happens, with the most significant variations observed at positions 58, 284, and 357, a result that could be expected in the light of the discussion above.

CONCLUSIONS

We have calculated the minimum free-energy path for the transformation between MC and CI in TrSA and in the quintuple mutant $TrSA_{5mut}$. The results were compared with those already available for TcTS. The comparison showed that the active site of $TrSA_{5mut}$ and TcTS hold the substrate in a similar way mainly due to positioning of residues Trp312 and Tyr119. However, both TrSA and $TrSA_{5mut}$ exhibit a higher degree of stabilization of the CI conformation than TcTS. Because of this fact, the barrier for the reverse reaction, a step required for trans-sialidase activity, becomes significantly higher, placing trans-sialylation at disadvantage against hydrolysis. These results provide an explanation for the lack of trans-sialidase activity of TrSA and the low activity detected in $TrSA_{5mut}$. Examination of the active site structures along the minimum free-energy path also reveals that the nucleophilic participation at the TS is much larger in TcTS than in TrSA and $TrSA_{5mut}$. This confirms previous studies suggesting that mutations aimed at increasing the mobility of the nucleophile are important to confer such activity. Based on this fact, two mutations were proposed for $TrSA_{5mut}$ to increase its nucleophile flexibility. Finally, by employing an energy decomposition analysis we contrasted the CI stabilization pattern for the active site residues in TcTS and $TrSA_{5mut}$. The comparison revealed that three residues are critical to provide high CI stabilization in $TrSA_{5mut}$. Two of them are different in TcTS and $TrSA_{5mut}$. Clearly they have to be mutated to obtain an enzyme with the ability to transfer sialic acid. An extra mutation was also proposed to change the CI stabilization pattern for the third residue.

According to the reasons given above five extra mutations were proposed to be introduced into $TrSA_{5mut}$. These mutations are: Ile36-Leu, Thr38-Ala, Phy58-Asn, Asp284-Gly, and Gly341-Ala. The resultant $TrSA_{10mut}$ was prepared *in silico*. Computations of the minimum free-energy path for $TrSA_{10mut}$ suggest that this mutant should bear a significantly increased trans-sialidase activity. Moreover, the nucleophilic participation at the TS, as well as the pattern of CI stabilization for key active site residues, are also alike in the two enzymes. Altogether, these results give a strong indication about the mutations required to provide TrSA with the capacity to transfer sialic acid. It remains to be seen if such mutant can be experimentally obtained and tested to confirm or refuse this proposal.

ACKNOWLEDGMENTS

The authors thank High-Performance Computing Center at the University of Florida for providing computational resources and Juan Bueren Calabuig, Santiago, and Johan F. Galindo for the corrections and suggestions made in this manuscript.

REFERENCES

1. Buscaglia CA, Campo VA, Frasch AC, Di Noia JM. *Trypanosoma cruzi* surface mucins: host-dependent coat diversity. Nat Rev Micro 2006;4:229–236.

2. Pereira ME, Zhang K, Gong Y, Herrera EM, Ming M. Invasive phenotype of *Trypanosoma cruzi* restricted to a population expressing trans-sialidase. Infect Immun 1996;64:3884–3892.
3. Pereira-Chioccola VL, Acosta-Serrano A, Correia de Almeida I, Ferguson MA, Souto-Padron T, Rodrigues MM, Travassos LR, Schenkman S. Mucin-like molecules form a negatively charged coat that protects *Trypanosoma cruzi* trypomastigotes from killing by human anti-alpha-galactosyl antibodies. J Cell Sci 2000;113:1299–1307.
4. Schenkman S, Eichinger D, Pereira M, Nussenzweig V. Structural and functional properties of *Trypanosoma* trans-sialidase. Annu Rev Microbiol 1994;48:499–523.
5. Yoshida N, Mortara RA, Araguth MF, Gonzalez JC, Russo M. Metacyclic neutralizing effect of monoclonal antibody 10D8 directed to the 35- and 50-kilodalton surface glycoconjugates of *Trypanosoma cruzi*. Infect Immun 1989;57:1663–1667.
6. Schenkman RP, Vandekerckhove F, Schenkman S. Mammalian cell sialic acid enhances invasion by *Trypanosoma cruzi*. Infect Immun 1993;61:898–902.
7. Schenkman S, Jiang M-S, Hart GW, Nussenzweig V. A novel cell surface trans-sialidase of *Trypanosoma cruzi* generates a stage-specific epitope required for invasion of mammalian cells. Cell 1991;65:1117–1125.
8. Belen Carrillo M, Gao W, Herrera M, Alroy J, Moore JB, Beverley SM, Pereira MA. Heterologous expression of *Trypanosoma cruzi* trans-sialidase in *Leishmania major* enhances virulence. Infect Immun 2000;68:2728–2734.
9. Mucci J, Hidalgo A, Mocetti E, Argibay PF, Leguizamón MS, Campetella O. Thymocyte depletion in *Trypanosoma cruzi* infection is mediated by trans-sialidase-induced apoptosis on nurse cells complex. Proc Natl Acad Sci USA 2002;99:3896–3901.
10. Muiá RP, Yu H, Prescher JA, Hellman U, Chen X, Bertozzi CR, Campetella O. Identification of glycoproteins targeted by *Trypanosoma cruzi* trans-sialidase, a virulence factor that disturbs lymphocyte glycosylation. Glycobiology 2010;20:833–842.
11. Henrissat B. A classification of glycosyl hydrolases based on amino acid sequence similarities. Biochem J 1991;280 (Pt 2):309–316.
12. Cantarel BL, Coutinho PM, Rancurel C, Bernard T, Lombard V, Henrissat B. The Carbohydrate-Active EnZymes database (CAZy): an expert resource for glycogenomics. Nucl Acids Res 2009;37 (Suppl 1):D233–D238.
13. Amaya MF, Buschiazzo A, Nguyen T, Alzari PM. The high resolution structures of free and inhibitor-bound *Trypanosoma rangeli* sialidase and its comparison with *T. cruzi* trans-sialidase. J Mol Biol 2003;325:773–784.
14. Sinnott ML. Carbohydrate chemistry and biochemistry. Cambridge: The Royal Society of Chemistry; 2007. pp 403–407.
15. Paris G, Cremona ML, Amaya MF, Buschiazzo A, Giambiagi S, Frasch AC, Alzari PM. Probing molecular function of trypanosomal sialidases: single point mutations can change substrate specificity and increase hydrolytic activity. Glycobiology 2001;11:305–311.
16. Yang J, Schenkman S, Horenstein BA. Primary ^{13}C and beta-secondary ^{2}H KIEs for trans-sialidase. A snapshot of nucleophilic participation during catalysis. Biochemistry 2000;39:5902–5910.
17. Watts AG, Damager I, Amaya ML, Buschiazzo A, Alzari P, Frasch AC, Withers SG. *Trypanosoma cruzi* trans-sialidase operates through a covalent sialyl-enzyme intermediate: tyrosine is the catalytic nucleophile. J Am Chem Soc 2003;125:7532–7533.
18. Pierdominici-Sottile G, Horenstein N, Roitberg A. A free energy study of the catalytic mechanism of *Trypanosoma cruzi* trans-sialidase. From the Michaelis complex to the covalent intermediate. Biochemistry 2011;50:10150–10158.
19. Buschiazzo A, Amaya MF, Cremona ML, Frasch AC, Alzari PM. The crystal structure and mode of action of trans-sialidase, a key enzyme in *Trypanosoma cruzi* pathogenesis. Mol Cell 2002;10:757–768.
20. Pontes-de-Carvalho LC, Tomlinson S, Nussenzweig V. *Trypanosoma rangeli* sialidase lacks trans-sialidase activity. Mol Biochem Parasitol 1993;62:19–25.
21. Paris G, Ratier L, Amaya MF, Nguyen T, Alzari PM, Frasch AC. A sialidase mutant displaying trans-sialidase activity. J Mol Biol 2005; 345:923–934.
22. Streicher H. Inhibition of microbial sialidases—what has happened beyond the influenza virus? Curr Med Chem: Anti-Infect Agents 2004;3:149–161.
23. Amaya MF, Watts AG, Damager I, Wehenkel A, Nguyen T, Buschiazzo A, Paris G, Frasch AC, Withers SG, Alzari PM. Structural insights into the catalytic mechanism of Trypanosoma cruzi trans-sialidase. Structure 2004;12:775–784.
24. Demir O, Roitberg AE. Modulation of catalytic function by differential plasticity of the active site: case study of *Trypanosoma cruzi* trans-sialidase and *Trypanosoma rangeli* sialidase. Biochemistry 2009;48:3398–3406.
25. Buschiazzo A, Tavares GA, Campetella O, Spinelli S, Cremona ML, Paris G, Fernanda Amaya M, Frasch AC, Alzari PM. Structural basis of sialyltransferase activity in trypanosomal sialidases. EMBO J 2000;19:16–24.
26. Smith LE, Eichinger D. Directed mutagenesis of the *Trypanosoma cruzi* trans-sialidase enzyme identifies two domains involved in its sialyltransferase activity. Glycobiology 1997;7:445–451.
27. Mitchell FL, Miles SM, Neres J, Bichenkova EV, Bryce RA. Tryptophan as a molecular shovel in the glycosyl transfer activity of *Trypanosoma cruzi* trans-sialidase. Biophys J 2010;98:L38–L40.
28. Case DA, Darden TA, Cheatham TE III, Simmerling CL, Wang J, Duke RE, Luo R, Crowley M, Walker R, Zhang W, Merz KM, Wang B, Hayik S, Roitberg A, Seabra G, Kolossvary I, Wong KF, Paesani F, Vanicek J, Wu X, Brozell SR, Steinbrecher T, Gohlke H, Yang LTC, Mongan J, Hornak V, Cui G, Mathews DH, Seetin MG, Sagui C, Babin V, Kollman AP. AMBER 10. San Francisco: University of California; 2008.
29. Jorgensen WL, Chandrasekhar J, Madura JD, Impey RW, Klein ML. Comparison of simple potential functions for simulating liquid water. J Chem Phys 1983;79:926–935.
30. Cornell WD, Cieplak P, Bayly CI, Gould IR, Merz KM, Ferguson DM, Spellmeyer DC, Fox T, Caldwell JW, Kollman PA. A second generation force field for the simulation of proteins, nucleic acids, and organic molecules. J Am Chem Soc 1995;117:5179–5197.
31. Hornak V, Abel R, Okur A, Strockbine B, Roitberg A, Simmerling C. Comparison of multiple Amber force fields and development of improved protein backbone parameters. Proteins: Struct Funct Bioinform 2006;65:712–725.
32. Basma M, Sundara S, Çalgan D, Vernali T, Woods RJ. Solvated ensemble averaging in the calculation of partial atomic charges. J Comput Chem 2001;22:1125–1137.
33. Kirschner KN, Woods RJ. Solvent interactions determine carbohydrate conformation. Proc Natl Acad Sci USA 2001;98:10541–10545.
34. Elstner M, Porezag D, Jungnickel G, Elsner J, Haugk M, Frauenheim T, Suhai S, Seifert G. Self-consistent-charge density-functional tight-binding method for simulations of complex materials properties. Phys Rev B 1998;58:7260–7268.
35. Seabra GM, Walker RC, Elstner M, Case DA, Roitberg AE. Implementation of the SCC-DFTB method for hybrid QM/MM simulations within the amber molecular dynamics package†. J Phys Chem A 2007;111:5655–5664.
36. Kruger T, Elstner M, Schiffels P, Frauenheim T. Validation of the density-functional based tight-binding approximation method for the calculation of reaction energies and other data. J Chem Phys 2005;122:114110–114115.
37. Woodcock HL, Hodoscek M, Brooks BR. Exploring SCC-DFTB paths for mapping QM/MM reaction mechanisms†. J Phys Chem A 2007;111:5720–5728.
38. Barnett CB, Naidoo KJ. Ring puckering: a metric for evaluating the accuracy of AM1, PM3, PM3CARB-1, and SCC-DFTB carbohydrate QM/MM simulations. J Phys Chem B 2010;114:17142–17154.
39. Biarnés X, Ardèvol A, Planas A, Rovira C, Laio A, Parrinello M. The conformational free energy landscape of β-D-glucopyranose.

Implications for substrate preactivation in β-glucoside hydrolases. J Am Chem Soc 2007;129:10686–10693.
40. Sindhikara DJ, Kim S, Voter AF, Roitberg AE. Bad seeds sprout perilous dynamics: stochastic thermostat induced trajectory synchronization in biomolecules. J Chem Theory Comput 2009;5:1624–1631.
41. Kumar S, Rosenberg JM, Bouzida D, Swendsen RH, Kollman PA. Multidimensional free-energy calculations using the weighted histogram analysis method. J Comput Chem 1995;16:1339–1350.
42. Torrie GM, Valleau JP. Nonphysical sampling distributions in Monte Carlo free-energy estimation: umbrella sampling. J Comput Phys 1977;23:187–199.
43. Lin Y-L, Gao J. Internal proton transfer in the external pyridoxal 5α-phosphate Schiff base in Dopa decarboxylase. Biochemistry 2009;49:84–94.
44. Pierdominici-Sottile G, Roitberg AE. Proton transfer facilitated by ligand binding. An energetic analysis of the catalytic mechanism of *Trypanosoma cruzi* trans-sialidase. Biochemistry 2010;50: 836–842.
45. Hensen C, Hermann CJ, Nam K, Ma S, Gao J, Holtje H. A combined QM/MM approach to protein-ligand interactions: polarization effects of the HIV-1 protease on selected high affinity inhibitors. Washington, DC, ETATS-UNIS: American Chemical Society; 2004. 8 p.
46. Chatfield DC, Eurenius PK, Brooks BR. HIV-1 protease cleavage mechanism: a theoretical investigation based on classical MD simulation and reaction path calculations using a hybrid QM/MM potential. J Mol Struct: Theochem 1998;423:79–92.
47. Cunningham MA, Ho LL, Nguyen DT, Gillilan RE, Bash PA. Simulation of the enzyme reaction mechanism of malate dehydrogenase. Biochemistry 1997;36:4800–4816.
48. Davenport RC, Bash PA, Seaton BA, Karplus M, Petsko GA, Ringe D. Structure of the triosephosphate isomerase-phosphoglycolohydroxamate complex: an analog of the intermediate on the reaction pathway. Biochemistry 1991;30:5821–5826.
49. Dinner AR, Blackburn GM, Karplus M. Uracil-DNA glycosylase acts by substrate autocatalysis. Nature 2001;413:752–755.
50. Garcia-Viloca M, Truhlar GD, Gao J. Reaction-path energetics and kinetics of the hydride transfer reaction catalyzed by dihydrofolate reductase. Washington, DC, ETATS-UNIS: American Chemical Society; 2003. 18 p.
51. Major DT, Gao J. A combined quantum mechanical and molecular mechanical study of the reaction mechanism and α-amino acidity in alanine racemase. J Am Chem Soc 2006;128:16345–16357.
52. Wong K-Y, Gao J. The reaction mechanism of paraoxon hydrolysis by phosphotriesterase from combined QM/MM simulations. Biochemistry 2007;46:13352–13369.